ISSN 1392–1320 MATERIALS SCIENCE (MEDŽIAGOTYRA). Vol. 29, No. 4. 2023

Synthesis and Determination of Al^{3+} in Chinese Herbs from Heilongjiang Province by Fluorescent Probe of Naphthalimide

Guang YANG [1], Yan LANG [2]*

[1] *Business Economics Research Institute of Harbin Commercial University, Harbin 150028, Heilongjiang Province, China*
[2] *Department of Rehabilitation Therapy, Wuyi University, Nanping 354301, Fujian Province, China*

https://doi.org/10.5755/j02.ms.33594

Received 9 March 2023; accepted 5 May 2023

We reported a new naphthalimide fluorescence probe M1[dimethyl 3, 3'-((2-((2-butyl-1, 3-dioxo-2, 3-dihydro-1H-benzo[de] isoquinolin-6-yl) amino) ethyl) azanediyl) dipropionate] with Al^{3+} fluorescence system. Its UV-visible absorption spectrum and fluorescence spectrum showed remarkable optical characteristics. The optimal experimental conditions, including reaction temperature, pH, and reaction time were investigated. This system possessed a good anti-interference ability toward the other 16 metal ions. The M1 shows good linearity with Al^{3+} concentration ($1 \times 10^{-6} \sim 15 \times 10^{-6}$ mol/L). The LOD (Limit of Detection) was 7.55×10^{-8} mol/L. It has good resistance to interference. It was excellently resistant to interferences. The complexation ratio between the M1 probe and Al^{3+} is 1:1. Furthermore, the binding mechanism was conjectured. We applied the constructed fluorescence system for the first time to the determination of Al^{3+} in Chinese herbal medicines, and fluorescence imaging in living cells.

Keywords: fluorescence probe, naphthalimide, Al^{3+}, construction and application.

1. INTRODUCTION

With the rapid development of economic construction in Heilongjiang and the gradual improvement of science and technology, the material living standard of the people has also improved a lot, but environmental problems have also come one after another. The discharge of industrial waste leads to a large accumulation of aluminum ions in the environment. Aluminum ions in acidic soils are toxic to plant roots, thereby inhibiting plant growth [1]. More seriously, aluminum ions that are enriched in the human body are difficult to be excreted and can adversely affect certain cellular tissues and the nervous system, which in turn can lead to various diseases [2, 3]. Therefore, it is particularly important to achieve the detection of aluminum ions in the environment and living organisms.

Due to the effects of metal ions on the environment and the human body, various detection methods have been investigated. For example, atomic fluorescence (AFS), atomic absorption (AAS), inductively coupled plasma (ICP), chemical titration, electrochemical analysis, and chromatograph [4–6]. Although these methods have the advantages of low detection limits and high sensitivity, they also have the disadvantages of expensive instruments, complicated operation, troublesome pre-treatment and long time-consuming. These problems are limiting the practical application of the above methods. Currently, fluorescent probes have received increasing attention from researchers due to their low detection limits, simplicity, low cost and instantaneous response, and a large number of organic fluorescent probes for metal ions have been synthesized. Many of these probes can be applied to qualitatively identify metal ions in cells and organisms [7–9]. Compared with traditional metal ion detection methods, fluorescent probes have the advantages of good selectivity, high sensitivity, low dependence on equipment, simple operation, and low detection limits. It plays an increasingly important role in bio-detection, ion monitoring [10–13], molecular monitoring [14–16], cell imaging [17–19], drug delivery [20, 21] and environmental monitoring [22, 23], etc.

The excellent photochemical and physical properties of naphthalimide derivatives have made them a hot topic in fluorescent probes for the detection of ions. Because of the presence of the electron-pulling "imide" group and the strong electron-donating group R_2, they constitute the electron transfer transition (ET) band, resulting in color changes and high fluorescence quantum yields. Researchers have designed different organic fluorescent probes by changing R_1, and R_2. These probes have the advantages of good selectivity, interference resistance, high sensitivity, large Stokes shift and high quantum yield of fluorescence, and are widely used in chemistry, medicine and environmental science [24].

A new Schiff base fluorescent probe NBP was synthesized and characterized by Zhang et al. [25]. The LOD of NBP toward Al^{3+} was 80 nM, and the binding ratio was 1:2. Besides, cell imaging experiments revealed NBP could serve as an indicator for monitoring Al^{3+} ions in living cells. Wang et al. [26] designed and synthesized a kind of naphthalimide probe NBPN, which process a significant selectivity toward Al^{3+} with a good linearity in the concentration range of $3 \sim 11$ μM. In 2019, CaifengDing's group [27] designed a probe DEHP to detect human serum albumin (HSA). before the addition of HSA, the aromatic ring of the probe was orthogonal to the plane, while after the addition of HSA, the TICT effect of the probe DEHP itself was suppressed and the aromatic ring was rotated, resulting in a red fluorescence in the probe response.

* Corresponding author. Tel.: +13644547989.
E-mail: *langyan@wuyiu.edu.cn* (Y. Lang)

FenglinWang's group [28] synthesized and designed a ratiometric fluorescence probe SN-N_3 based on naphthalimide and aniline, and after the N_3 group was attacked by H_2S to change N3 to the amino group, aniline was separated from the probe SN-N3. The fluorescence changed from blue to green, and ratiometric fluorescence detection was achieved. 2017 Qiao [29] group designed fluorescent probes to enhance the fluorescence intensity and photostability of naphthalimide dyes, localize and detect proteins based on naphthalimide fluorophores with a combination of theoretical and experimental approaches. A series of naphthalimide fluorescence-enhanced fluorescent probes were synthesized, and the method enables wash-free fluorescence imaging of target proteins in the nucleus and mitochondria, avoiding cell damage and achieving a high signal-to-noise ratio for the detection of target proteins in living cells.

In our work, we reported a new fluorescence system fluorescence probe M1-Al^{3+} based on naphthalimide. Its fluorescence spectrum and ultraviolet spectrum characteristics show that the probe has great application prospects in optical detection. Its anti-interference ability in complex environments endowed it with excellent detection ability. In addition, the ligand ratio of the system helped to explain its principle. To investigate the application of the probe, we applied the system to the determination of Al^{3+} content in herbal medicines, provided technical formulas and a reference basis for the quality control of herbal medicines, and applied it to the study of living cell imaging.

2. EXPERIMENTAL DETAILS

Instruments: fluorescence spectrophotometer (970CRT, Shanghai), acidity meter (pHS-3C, Sedolis, Germany), ultraviolet spectrophotometer (UV-2550, Suzhou Beirui), electronic balance (JD100-3A, Zhengzhou Wanbo).

Reagents: the reagents used in this study were analytical grade: zinc chloride ($ZnCl_2$), calcium chloride ($CaCl_2$), potassium chloride (KCl), methanol (CH_3OH), magnesium chloride ($MgCl_2$), cobalt chloride hexahydrate ($CoCl_2{\cdot}6H_2O$), sodium chloride (NaCl), nickel chloride hexahydrate ($NiCl_2{\cdot}6H_2O$), manganese chloride ($MnCl_2$), ferrous chloride ($FeCl_2$), cadmium chloride ($CdCl_2$), aluminum chloride ($AlCl_3$), ferric chloride hexahydrate ($FeCl_3{\cdot}6H_2O$), cupric chloride ($CuCl_2$), sodium hydroxide (NaOH).

Instruments: NEXUS-670 FT-IR spectrometer, Nicorette Corporation, USA; AV-400 Nuclear Magnetic Resonance Spectrometer, Bruker, Germany; DZF-6020A vacuum drying oven, Shanghai Kuntian Co; JD100-3A precision electronic balance, Zhengzhou Wanbo Company; HWS-12 electrothermal constant temperature water bath, Shanghai Yiheng Company.

Synthesis of Fluorescent Probe M1: compound 1 was synthesized by taking 6 g of 4-bromo-1,8 naphthalic anhydride, 150 mL of anhydrous ethanol, and 6.24 mL of L1-aminobutane in a three-necked round-bottom flask, passing nitrogen into the flask, and stirring and heating to reflux for 12 h. After the reaction was completed and cooled to room temperature, the reaction was poured into a beaker with ice water, and a precipitate appeared at the bottom of the beaker, which was filtered to obtain a light-yellow solid, washed with distilled water three times, and then placed in a vacuum drying oven. The product was washed with distilled water 3 times and then put into a vacuum drying oven. The dried product was recrystallized with anhydrous ethanol to obtain light yellow powder compound 1.

Compound 2 was synthesized by adding 1 g of compound 1 and 12.2 g of ethylenediamine to a single bottom flask and refluxing with stirring for 4 h. After the reaction, the solution was cooled to room temperature. The cooled solution was poured into a beaker with ice water and a large amount of precipitate appeared in the beaker, which was filtered to obtain a yellow solid.

The M1 probe was synthesized by adding 2 g of compound 2 and 80 mL of anhydrous ethanol to a single bottom flask, and the flask was placed in a water bath and stirred vigorously until compound 2 was completely dissolved and the heating was stopped. After the solution cooled completely, 5.843 g of methyl acrylate was slowly added and stirred for 48 h. The filter cake obtained by filtration was washed three times with anhydrous ethanol, and the washed filter cake was dried in a vacuum drying oven for 24 h. The yellow solid was obtained as the probe M1. The synthetic pathway is shown in Fig. 1.

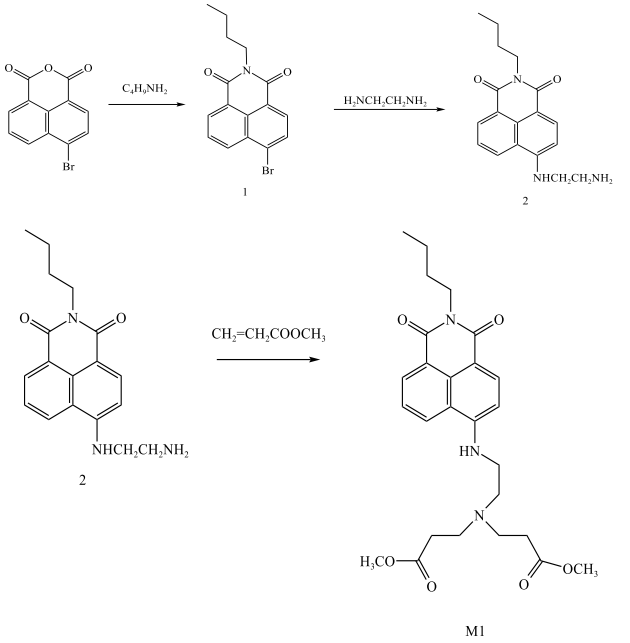

Fig. 1. Synthesis pathway of M1 probes

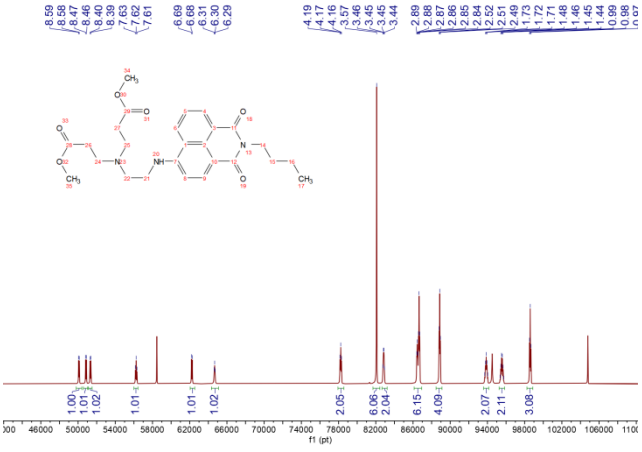

Fig. 2. ^{1}H-NMR spectrum of M1

Nuclear magnetic resonance characterization atlas: 1H NMR (600 MHz, $CDCl_3$) δ: 8.59 (*d*, J = 7.3 Hz, 1H), 8.47 (*d*, J = 8.4 Hz, 1H), 8.39 (*d*, J = 8.4 Hz, 1H), 7.62 (*t*,

J = 7.8 Hz, 1H), 6.68 (*d*, J = 8.4 Hz, 1H), 6.30 (*t*, J = 4.6 Hz, 1H), 4.17 (*t*, J = 7.7 Hz, 2H), 3.57 (*s*, 6H), 3.45 (*q*, J = 5.1 Hz, 2H), 2.92–2.78 (*m*, 6H), 2.51 (*t*, J = 6.4 Hz, 4H), 1.72 (*p*, J = 7.7 Hz, 2H), 1.46 (*h*, J = 7.4 Hz, 2H), 0.98 (*t*, J = 7.4 Hz, 3H). The NMR hydrogen spectrum of M1 is shown in Fig. 2.

Preparation of sample solution: to obtain probe sample solution (1×10^{-5} mol·L^{-1}), M1 probe (9.6 mg) was dispersed in anhydrous methanol (10 mL), then diluted 200 times with MeOH:H_2O = 2:1 (V:V).

To obtain a metal ion solution (1×10^{-2} mol·L^{-1}), anhydrous aluminium chloride (133.34 mg) was dispersed in distilled water (10 mL), then diluted 10 times with deionized water. Other metal ions (Cu^{2+}, Co^{2+}, K^{+}, Mg^{2+}, Mn^{2+}, Pb^{2+}, Zn^{2+}, Fe^{2+}, Na^{+}, Ca^{2+}, Ni^{2+}, Cd^{2+}, Fe^{3+}, Sn^{2+}, Hg^{2+}) are also prepared to 1×10^{-2} mol·L^{-1} in the similar way.

Spectral experimental method: 11 equivalents of Al^{3+} solution were pipetted into the probe sample solution, mixed well and left to stand. The fluorescence spectrum in a 1 cm cuvette (excitation wavelength 400 nm, sensitivity 1, similarly hereinafter). The UV absorption spectrum was measured in a cuvette using anhydrous methanol as the reference solution. Meanwhile, another blank probe sample solution was tested in the same method.

Selectivity of probe to metal ions: the same volume of probe sample solution with the concentration were separately pipetted into 16 specimen tubes. 11 equivalents of the metal ion solution (Cu^{2+}, Co^{2+}, K^{+}, Mg^{2+}, Mn^{2+}, Pb^{2+}, Zn^{2+}, Fe^{2+}, Na^{+}, Ca^{2+}, Ni^{2+}, Cd^{2+}, Hg^{2+}, Fe^{3+}, Al^{3+}, Sn^{2+}) to each of them with a pipette, mixed well and left to stand. Then, the UV absorption spectra and the fluorescence spectrum of the solutions in each of the 16 specimen tubes were tested, respectively.

Titration of Al^{3+} by a probe: under the optimal experimental conditions, different equivalents of Al^{3+} solution was pipetted into the probe sample solution, shaken well, and the fluorescence emission spectra and the UV absorption spectra were tested, respectively.

Anti-interference experiment: 15 groups of probe sample solutions were added with 11 equivalents of Al^{3+} solution, and then 11 equivalents of interfering metal ion solution (Cu^{2+}, Co^{2+}, K^{+}, Mg^{2+}, Mn^{2+}, Pb^{2+}, Zn^{2+}, Fe^{2+}, Na^{+}, Ca^{2+}, Ni^{2+}, Cd^{2+}, Hg^{2+}, Fe^{3+}, Al^{3+}, Sn^{2+}) were added separately. After mixing well and leaving to stand, the samples' fluorescence spectrum was tested.

Plotting of standard curve: different equivalents of Al^{3+} metal solutions were added to the probe sample solution, mixed well, left to stand, and the fluorescence intensity was measured separately.

Experimental condition investigation: two sets of probe sample solutions were taken, and 11 equivalents of Al^{3+} solution were added to one set. They were measured separately by fluorescence spectrophotometer within the temperature of 5 to 65 °C (interval of 5 °C).

Two sets of probe sample solutions were taken, and 11 equivalents of Al^{3+} solution were added to one set. The pH was adjusted from 1 to 12 with NaOH solution and HCl solution. They were measured separately by fluorescence spectrophotometer within 0 to 90 min (interval of 5 min).

Ligand ratio experiments: the total concentration of the probe and Al^{3+} in mixed solution was kept constant at

5×10^{-5} mol/L. The fluorescence emission spectroscopy was measured while the molar ratio of a probe to Al^{3+} in the mixed solution continuously changed from 0.1 to 0.9.

Determination of LOD: the fluorescence intensity of the blank probe solution was measured 11 times in parallel. Thus, the standard deviation was calculated, and LOD was calculated using the formula LOD = 3δ/k.

Methodological examination. Precision: 10 groups of mixed solutions of probes and Al^{3+} with the same concentration were accurately measured and detected separately by fluorescence spectrophotometer.

Accuracy: three groups of fluorescent system solutions with Al^{3+} concentrations of 4, 6 and 13 (10^{-6} mol/L) were taken, and the fluorescence intensity of each group was measured three times. The recovery was calculated according to the measured and actual concentrations. The relative standard deviation calculated by recovery is used to examine the accuracy of the method.

Reversibility study of fluorescent systems: the fluorescence spectrum of the probe sample solution was recorded when 11 equivalents of Al^{3+} solution and 22 equivalents of EDTA aqueous solution were added, respectively. Finally, excessive Al^{3+} was added and the fluorescence spectrum was recorded.

Application research. Sample detection: the herbal medicines Panacis Quinquefolii Radix (PQR) and Paeoniae Radix Alba (PRA) got properly cleaned, cut, dried and ground, respectively. Four parts of 0.6 g powder got weighed. After being digested by acid and heat, the excess acid was removed. and another blank sample was labeled. The volume was adjusted to 50 mL with deionized water (pH = 7). Then the content of Al^{3+} was measured 3 times in a row.

Cell culture conditions: Dulbecco's modified eagle medium added 10 % Fetal Bovine Serum, the atmosphere made up of clean air: CO_2 (95:5). Cell imaging: HeLa cells were immersed in the probe sample solution, incubated for 30 min, rinsed twice, and recorded by fluorescence microscopy. Then, saturated Al^{3+} was infunded and incubated for 30 minutes, rinsed twice, and the cells got recorded by fluorescence microscopy.

Cytotoxicity assay: different concentrations of M1 probe solution were added dropwise to the HeLa cells after incubation, and the cells were incubated for 24 h. MTT (thiazole blue) reagent was added and incubated for 4 h. The survival rate of the cells was observed on an enzyme marker.

Cell fluorescence imaging experiments: HeLa cells were treated with M1 probe solution at a concentration of 1×10^{-5} mol/L, incubated for 30 min, rinsed twice with culture medium, observed by fluorescence microscopy, and fluorescence micrographs were taken. Subsequently, saturated equivalents of Al^{3+} solution were added to the probe treated cells, incubated for 30 min, rinsed twice with culture medium, observed by fluorescence microscopy, and photographed fluorescence micrographs.

3. RESULTS AND DISCUSSION

3.1. Spectral experimental

As shown in Fig. 3, the pure probe solution has a weak peak at 541 nm. After adding Al^{3+} solution, it shifted to 526 nm and its intensity increased. It indicated that the Al^{3+} fluorescent system had been successfully built.

Fig. 4 shows the pure probe solution has three peaks at 439 nm, 259 nm, and 282 nm. After adding Al^{3+} solution, the peaks at 439 nm and 282 nm shifted to 526 nm and 274 nm,

respectively, and their intensities decreased. It is inferred that the Al^{3+} fluorescent system had been successfully built.

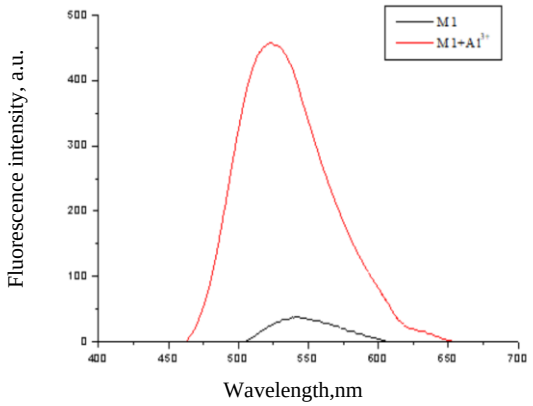

Fig. 3. Fluorescence response of M1 and Al^{3+} fluorescence systems

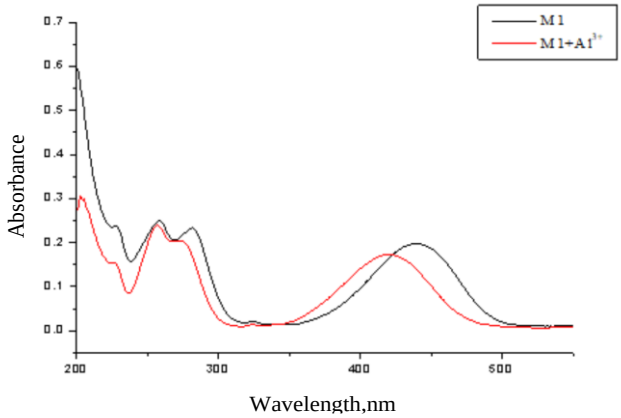

Fig. 4. UV-Vis absorption response of the system and probe M1

3.2. Selectivity of probe to metal ions

Fig. 5 shows, after separately adding ions (Cu^{2+}, Co^{2+}, K^{+}, Mg^{2+}, Mn^{2+}, Pb^{2+}, Zn^{2+}, Fe^{2+}, Na^{+}, Ca^{2+}, Ni^{2+}, Cd^{2+}, Hg^{2+}, Fe^{3+}, Al^{3+}, Sn^{2+}) to the probe solution. After adding Al^{3+}, the original peak at 541 nm shifted to 526 nm and increased significantly in intensity. After adding Al^{3+}, the original fluorescent peak of 541 nm shifted to 525 nm. The fluorescence peak responses were weak when other metal ions were added, and the fluorescence emission spectrums had no obvious change. It reveals that the M1 probe has good selectivity only for Fe^{3+} and Al^{3+}. Additionally, probe selectivity for Al^{3+} is superior to that for Fe^{3+} [30,31].

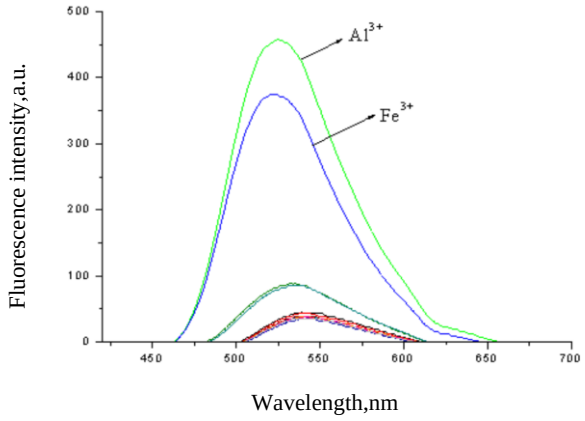

Fig. 5. Fluorescence response of different metal ions interacting with M1

Fig. 6 shows, after separately adding ions (Cu^{2+}, Co^{2+}, K^{+}, Mg^{2+}, Mn^{2+}, Pb^{2+}, Zn^{2+}, Fe^{2+}, Na^{+}, Ca^{2+}, Ni^{2+}, Cd^{2+}, Hg^{2+}, Fe^{3+}, Al^{3+}, Sn^{2+}) to the solution, the peaks of the fluorescence system with Fe^{3+} and Al^{3+} showed significant changes, while that with other ions almost never changed. After adding Al^{3+}, the peaks of probe at 439 nm and 282 nm shifted to 420 nm and 274 nm, respectively, and their intensities decreased. After adding Fe^{3+}, the peaks of probe at 439 nm and 282 nm disappeared and a new appeared at 367 nm. It reveals that the M1 probe has good selectivity only for Fe^{3+} and Al^{3+}. Additionally, probe selectivity for Al^{3+} is superior to that for Fe^{3+} [32].

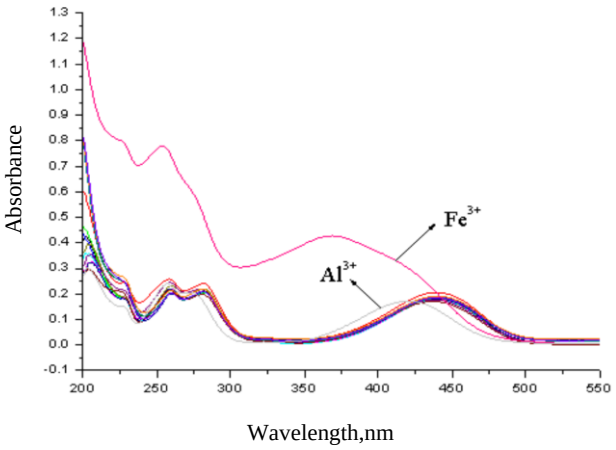

Fig. 6. UV absorption response of different metal ions interacting with M1

3.3. Titration of Al^{3+} by a probe

As shown in Fig. 7, when the Al^{3+} concentration increased, the peak shifted from 541 nm to 526 nm, and increased significantly in intensity. Once the Al^{3+} reached 11 equivalents, the fluorescence peak was essentially unchanged, indicating that the binding of the probe and Al^{3+} reaches saturation.

Fig. 8 shows, with the rise of Al^{3+} the peak at 439 nm and 282 nm shifted to 420 nm and 274 nm, respectively, and their intensities decreased. Once Al^{3+} reached 11 equivalents, the peaks of the fluorescent system were basically unchanged, indicating that the binding of the probe and Al^{3+} reaches saturation.

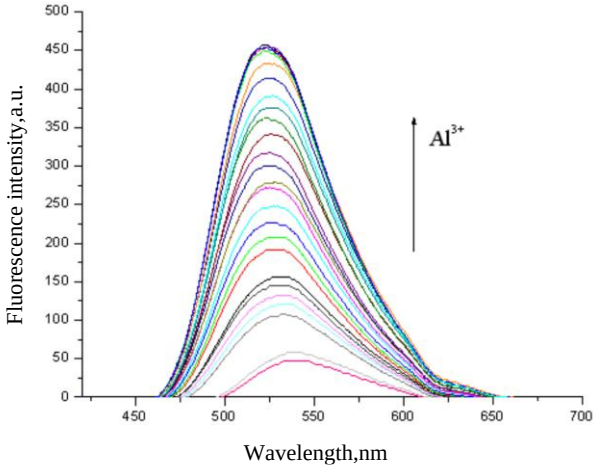

Fig. 7. Fluorescence titration response under different concentrations of Al^{3+}

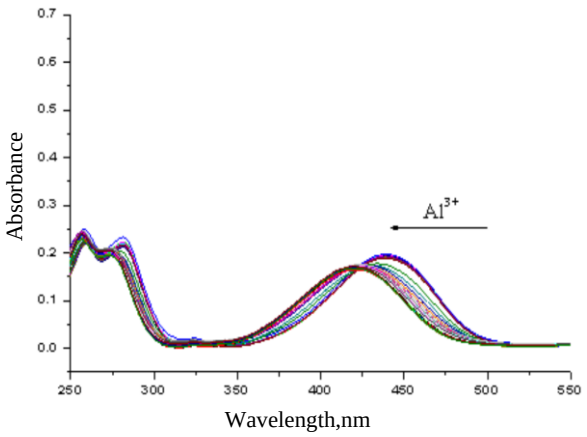

Fig. 8. UV titration response under different concentrations of Al^{3+}

3.4. Anti-interference experiment

Since the identification saturation amount of Al^{3+} is 11 equivalents, 11 equivalents of interfering ions were chosen for the interference test. Fig. 9 shows that the intensity of the system was not obviously influenced by interference ions, which indicates that the system has good anti-interference [33]. It reveals that the probe is sensitive to Al^{3+} and may detect Al^{3+} in complex environments [34, 35].

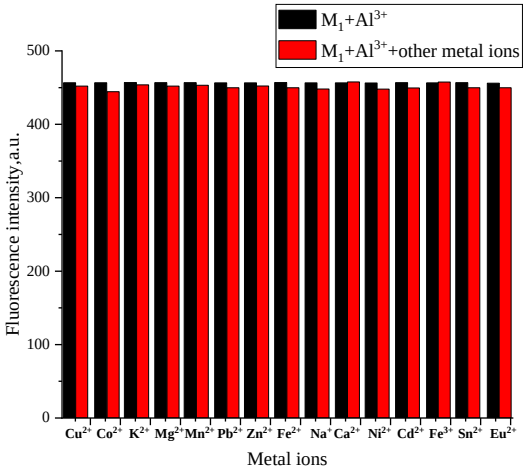

Fig. 9. Effects of interfering ions on fluorescence systems

3.4. Plotting of calibration curve

The intensity of the system rose in pace with the thickening of Al^{3+}. The difference of fluorescence intensity change

ΔF (F-F_0) was used as the vertical coordinate and the concentration of Al^{3+} was used as the horizontal coordinate in Fig. 10. Within 2.4×10^{-5} to 11×10^{-5} mol/L, the linear relationship between fluorescence intensity and Al^{3+} concentration can be expressed by formula:

$$y = 3.5552x + 31.248,\ R^2 = 0.9982. \quad (1)$$

3.5. Experimental condition investigation

The effect of temperature on the system was tested among 5 ~ 65 °C. Fig. 11 shows that the intensities of the pure probe and the system are stable in the range of 20 ~ 35 °C. Then 25 °C was set as the fluorescence system's optimal reaction temperature.

As shown in Fig. 12, the effect of pH variation on the fluorescence intensity was investigated. The intensity of pure probe was enhanced during 1 ~ 3, tended to stabilize between 6 ~ 8, gradually increased during 4 ~ 7, and reached a maximum at 7. Therefore, pH = 7 was determined as the optimum pH condition.

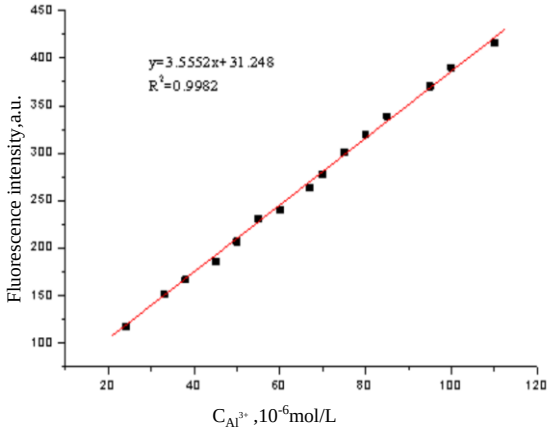

Fig. 10. Calibration curve

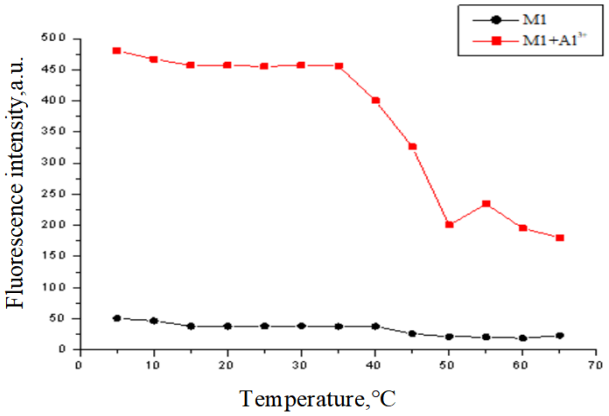

Fig. 11. Fluorescence response under different reaction temperatures

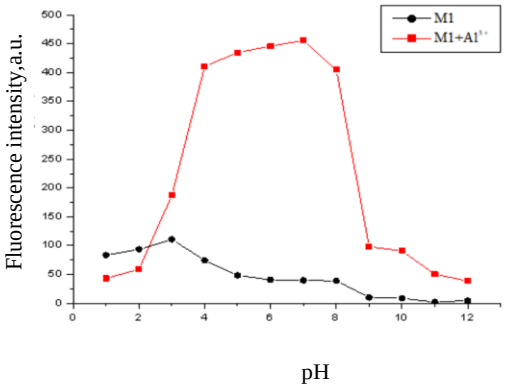

Fig. 12. Fluorescence response under different pH

The intensities of the pure probe and system were investigated within 0 to 90 min (interval of 5 min). Once the reaction time reaches 10 minutes, the fluorescence intensity of the system reaches its maximum value and stabilizes in Fig. 13. For a complete response, the optimal response time was set as 15 minutes.

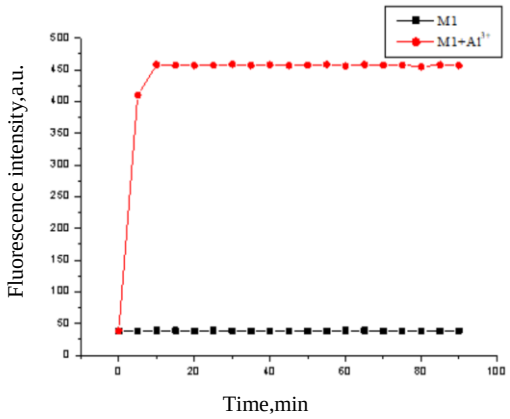

Fig. 13. Fluorescence response under different reaction times

3.6. Ligand ratio experiments

To investigate the reaction mechanism of the probe with aluminum ions, we explore and verify it by measuring the binding ratio of the probe (Fig. 14). The complex ratio of metal ions was first determined by measuring the binding ratio of the probe to determine the complex ratio of metal ions in the complex. After keeping the sum of probe concentration and Al^{3+} concentration at 5×10^{-5} mol/L, the Al^{3+} content varied uniformly between 0 and 1. The maximum fluorescence emission was observed when the molar ratio molar fraction in the Al^{3+} fluorescent system was 0.5. This suggests a stoichiometric ratio of 1:1 for Al^{3+}, further supporting our speculation [36].

The binding mechanism is shown in Fig. 15: Al^{3+} ligates with N and O, this inhibits photo-induced e^- transfer and promotes charge transfer inside the molecule, thus enhancing the fluorescence recovery of probe M1 [37, 38].

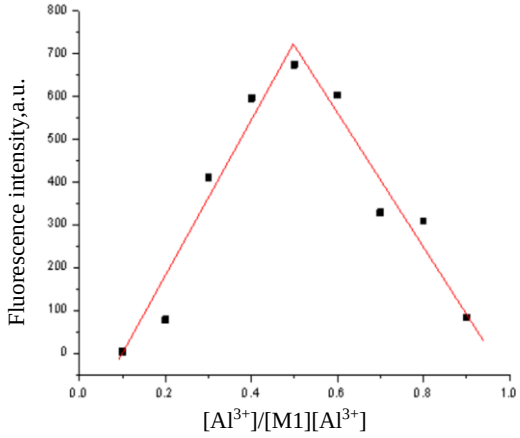

Fig. 14. The binding ratio curve

3.7. Determination of LOD

The blank probe solution was measured 11 times in parallel to record the fluorescence intensity, shown in Fig. 16. From the calculation, $\delta = 0.44$. From the equation $LOD = 3\delta/k$, the detection limit of the M1 probe for Al^{3+} was calculated to be 3.71×10^{-7} mol/L, close to that of Yadav et al. and Biswas et al. [39].

3.8. Methodological examination

Precision: as shown in Table 1, the relative standard deviation (RSD) of 10 groups with the same concentration is 1.03 %, below 5 %. It revealed that the constructed system was of good accuracy.

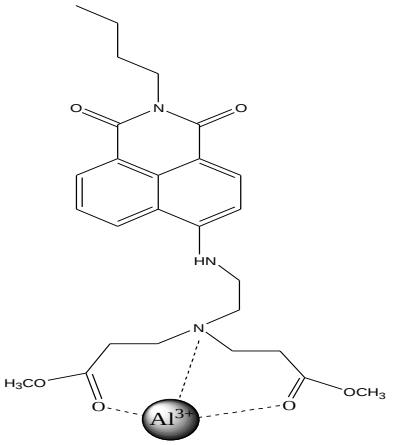

Fig. 15. The possible binding mechanism of probe M1 to Al^{3+}

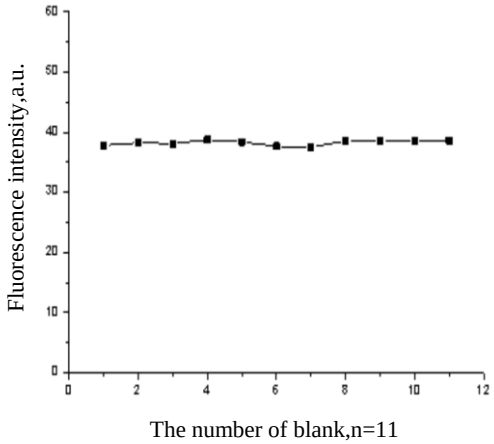

Fig. 16. Fluorescence response of the blank sample

Table 1. The precision results of the probe M1

Experiment times	$\triangle F$ (F-F_0)	$\triangle F$ average value	RSD, %
1	387.80	389.34	1.03
2	385.62		
3	383.28		
4	390.91		
5	393.65		
6	386.63		
7	393.12		
8	387.73		
9	388.49		
10	396.20		

Accuracy: Table 2 shows the recovery of the three groups' systems have RSD of less than 1.56 %, 0.92 %, 1.21 % and 1.09 %, respectively. The detection of the system had a higher precision.

3.9. Reversibility study of a fluorescent system

Reversibility is a crucial property of the fluorescent system. To verify the reversible reaction between Al^{3+} and the probe molecule, this paper chose to add EDTA aqueous solution to the constructed Al^{3+} fluorescent system. In Fig. 17, the intensity significantly decreased after mixing an adequate EDTA into the system.

Table 2. The accuracy results of the probe M1

Concentration, 10^{-5} mol/L	Recovery, %	Recovery mean ± *SD*/%	RSD, %
4	99.91	98.23 ± 1.53	1.56
	96.93		
	97.85		
	99.70		
7	101.11	100.98 ± 1.22	1.21
9	102.13	98.49 ± 1.07	1.09
	99.63		
	98.32		
	97.51		

Its mechanism can be expounded: EDTA separates Al^{3+} from the system and combined with it. Then, the fluorescence intensity recovers as excessive Al^{3+} is added. Thus, the recognition of Al^{3+} by the probe is highly reversible.

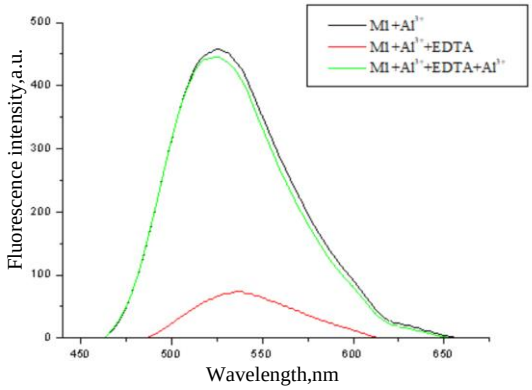

Fig. 17. Reversibility experiment of M1 and Al^{3+} fluorescence system

3.10. Application research

Sample Detection: Al^{3+} in Traditional Chinese Medicines was determined by this fluorescence system. Table 3 shows that the recoveries were 99.43 % ~ 100.39 % and 98.93 % ~ 99.85 %, respectively, with RSDs less than 2 %. It indicates that the fluorescence system can be used to determine the Al^{3+} content in the herb medicines PQR and PRA.

Table 3. Sample measurement results (n = 8)

Sample	Amount added, 10^{-6} mol/L	Recovery, 10^{-6} mol/L	Rate of recovery, %	RSD, % (n = 3)
PQR	0	–	–	–
PQR	30	29.83	99.43	1.36
PQR	60	59.75	99.58	1.64
PQR	100	100.39	100.39	1.77
PRA	0	–	–	–
PRA	30	29.79	99.3	1.23
PRA	60	59.91	99.85	1.1
PRA	100	98.93	98.93	1.17

Cell imaging: the cytotoxicity of M1 was measured by the MTT method. Four concentrations of M1 probe were taken separately for the experiment, and the cell survival rate was calculated using enzyme marker analysis. HeLa cells treated by the M1 probe of 5, 10, 15, 20 (10^{-5} mol/L) still had high survival rates of 99.57 %, 98.33 %, 95.23 % and 93.8 % in Fig. 18, respectively. It reveals that the probe has low biological toxicity for intracellular experiments.

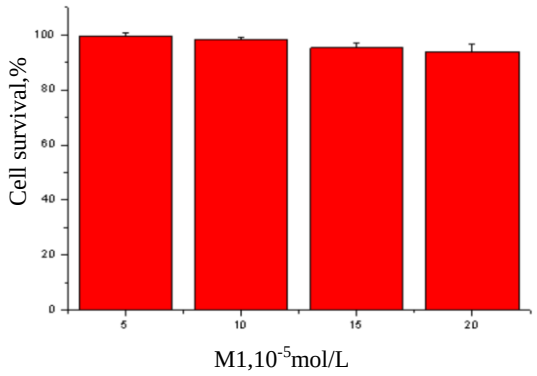

Fig. 18. Cytotoxicity assay of M1 probe

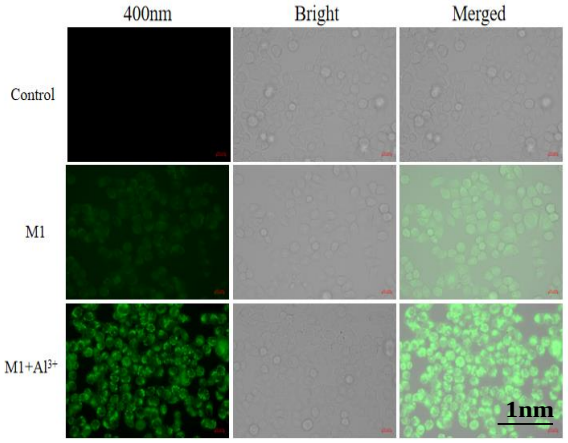

Fig. 19. Cell imaging experiment

In Fig. 19, the control set has no autofluorescence from the intrinsic fluorophores in the cells. Under the fluorescence microscope, the fluorescence response of the group treated with the probe was low, while that of the group treated with Al^{3+} and the probe was extremely strong. The results showed that the probe could pass through the living cell membrane, which can be applied to detect Al^{3+} in vitro and in vivo [40, 41].

4. CONCLUSIONS

In our work, we successfully constructed a kind of Al^{3+} fluorescent system, and its fluorescence spectrum and UV spectral properties were investigated. successfully constructed. With the addition of Al^{3+}, the peak position and peak intensity in fluorescence and UV spectra have changed significantly. The optimal experimental conditions were examined: pH = 7, optimum reaction time 15 min, and optimum reaction temperature 25 °C. The ligand ratio of the probe to Al^{3+} was 1:1. The fluorescence system has a strong anti-interference ability to 16 metal ions (Cu^{2+}, Co^{2+}, K^{+}, Mg^{2+}, Mn^{2+}, Pb^{2+}, Zn^{2+}, Fe^{2+}, Na^{+}, Ca^{2+}, Ni^{2+}, Cd^{2+}, Hg^{2+}, Fe^{3+}, Al^{3+}, Sn^{2+}). The detection limit for Al^{3+} reached 3.71×10^{-7} mol/L, with good linearity from 2.4×10^{-5} to 11×10^{-5} mol/L. The probe has also been successfully used in the detection of Al^{3+} in traditional Chinese medicines, providing guidance and a scientific basis for the detection of metal ions in foods and herbal medicines. The imaging in Haila cells shows that the probe has broad prospects for real-time monitoring of metal ions inside and outside the organism.

Acknowledgments

This work was financially supported by the National Social Science Foundation of China in 2022: Research on Traditional Phenological Calendar of Ethnic Minorities along the Heilongjiang River (Project No.: 22BMZ074).

REFERENCES

1. **Mark, C., Graeme, P.** Simultaneous Measurement of Exchangeable Al and Other Cations in Acidic Soils *Soil Research* 56 (5) 2018: pp. 114 – 117. https://doi.org/10.1071/sr18049
2. **Zhao, Y., Pogue, A.I., Alexandrov, P.N., Butler, L.G., Li, W.H., Jaber, V.R., Lukiw, W.J.** Alteration of Biomolecular Conformation by Aluminum-Implications for Protein Misfolding Disease *Molecules* 27 (16) 2022: pp. 5123. https://doi.org/10.3390/molecules27165123
3. **Yokel, R.A., Hicks, C.L., Florence, R.L.** Aluminum Bioavailability from Basic Sodium Aluminum Phosphate, an Approved Food Additive Emulsifying Agent, Incorporated in Cheese Food and Chemical Toxicology: An International Journal Published for the British Industrial Biological Research Association 46 (6) 2008: pp. 2261 – 2266. https://doi.org/10.1016/j.fct.2008.03.004
4. **Gagliano-Candela, R., Colucci, A.P., Napoli, S.** Determination of Firing Distance. Lead Analysis on the Target by Atomic Absorption Spectroscopy (AAS) *Journal of Forensic Sciences* 53 (2) 2008: pp. 321 – 324. https://doi.org/10.1111/j.1556-4029.2008.00668.x
5. **Deep, B., Balasubramanian, N., Nagaraja, K.S.** Spectrophotometric Determination of Cyanide Based on Berthelot reaction *Analytical Letters* 36 (13) 2003: pp. 2865 – 2874. https://doi.org/10.1081/al-120025261
6. **Herzog, F., Kahraman, A., Boehringer, D., Mak, R, Bracher, A., Walzthoeni, T., Leitner, A., Beck, M., Hartl, F.U., Ban, N., Malmström, L., Aebersold, R.** Structural Probing of a Protein Phosphatase 2A Network by Chemical Cross-linking and Mass Spectrometry *Science* 337 (6100) 2012: pp. 1348 – 1352. https://doi.org/10.1126/science.1221483
7. **Liu, H., Zhang, B., Tan, C., Cao, J.K., Tan, Y., Jiang, Y.Y.** Simultaneous Bioimaging Recognition of Al^{3+} and Cu^{2+} in Living-cell, and Further Detection of Fand S^{2-} by a Simple Fluorogenic Benzimidazole-based Chemosensor *Talanta* 161 2016: pp. 309 – 319. https://doi.org/10.1016/j.talanta.2016.08.061
8. **Rahman, F.U., Ali, A., Khalil, S.K., Guo, R., Zhang, P., Wang, H., Li, Z.T., Zhang, D.W.** Tuning Sensitivity of a Simple Hydrazone for Selective Fluorescent "Turn on" Chemo-sensing of Al^{3+} and its Application in Living Cells Imaging *Talanta* 164 2017: pp. 307 – 313. https://doi.org/10.1016/j.talanta.2016.10.085
9. **Peng, L., Zhou, Z., Wang, X., Wei, R.R., Li, K., Xiang, Y., Tong, A.J.** A Ratiometric Fluorescent Chemosensor for Al^{3+} in Aqueous Solution Based on Aggregation-induced Emission and its Application in Live-cell Imaging *Analytica Chimica Acta* 829 2014: pp. 54 – 59. https://doi.org/10.1016/j.aca.2014.04.046
10. **Shen, K.S., Mao, S.S., Shi, X.K., Wang, F., Xu, Y.L.** Characterization of a highly Al^{3+}-selective Fluorescence Probe Based on Naphthalimide-Schiff Base and its Application to Practical Water Samples Luminescence: The Journal of Biological and Chemical Luminescence 33 (1) 2018: pp. 54 – 63. https://doi.org/10.1002/bio.3372
11. **Shen, K., Mao, S., Shi, X., Aderinto, S.O., Xu, Y., Wu, H.** Development of a New 4-amino-1, 8-naphthalimide Derivative as a Fluorescent Probe for Monitoring the Divalent Copper Ion *Journal of Applied Spectroscopy* 85 (4) 2018: pp. 665 – 672. https://doi.org/10. 1007 /s10812-018-0702-9
12. **Chen, Z., Wang, L., Zou, G., Tang, J., Cai, X., Teng, M., Chen, L.** Highly Selective Fluorescence Turn-on Chemosensor Based on Naphthalimide Derivatives for Detection of copper(II) Ions *Spectrochimica Acta Part A: Molecular and Biomolecular Spectroscopy* 105 2013: pp. 57 – 61. https://doi.org/10.1016/j.saa.2012.12.005
13. **Yadav, S., Rajpurohit, D., Dash, S.R., Bhojani, G., Chatterjee, S., Paital, A.R.** Hybrid Material for Ferric Ion Detection & Remediation: Exceptional Selectivity & Adsorption Capacity with Biological Applications *Microporous and Mesoporous Materials* 338 2022: pp. 111945. https://doi.org/10.1016/j.micromeso.2022.111945
14. **Wang, Y., Huang, C., Jia, N.** Molecular Fluorescent Probe for Monitoring Cellular Microenvironment and Active Molecules *Progress in Chemistry* 32(Z1) 2020: pp. 204 – 218. https://doi.org/10.1021/acsmacrolett.0c00660
15. **Oshchepkov, A.S., Oshchepkov, M.S., Oshchepkova, M.V., Al-Hamry, A., Kanoun, O., Kataev, E.A.** Naphthalimide-based Fluorescent Polymers for Molecular Detection *Advanced Optical Materials* 9 (6) 2021: pp. 2001913. https://doi.org/10.1002/adom.202001913
16. **Geraghty, C., Wynne, C., Elmes, R.B.P.** 1, 8-Naphthalimide Based Fluorescent Sensors for Enzymes *Coordination Chemistry Reviews* 437 2021: pp. 213713. https://doi.org/10.1016/j.ccr.2020.213713
17. **Lei, S.R., Meng, X., Wang, L.Z., Zhou, J.H., Qin, D.W., Duan, H.D.** A Naphthalimide-Based Fluorescent Probe for the Detection and Imaging of Mercury Ions in Living Cells *ChemistryOpen* 10 (11) 2021: pp. 1116 – 1122. https://doi.org/10.1002/open.202100204
18. **Liu, F., Shen, Y.C., Chen, S., Yan, G.P., Zhang, Q., Guo, Q.Z., Gu, Y.T.** Tumor‐Targeting Fluorescent Probe Based on 1, 8‐naphthalimide and Porphyrin Groups *Chemistry Select* 5 (26) 2020: pp. 7680 – 7684. https://doi.org/10.1002/slct.202001340
19. **Ren, J., Wang, L., Guo, R., Tang, Y., Zhou, H., Lin, W.** A Naphthalimide-based Fluorescent Probe for Detecting Intracellular pH and Its Biological Imaging Application *Acta Chimica Sinica* 79 (01) 2021: pp. 87 – 92. https://doi.org/10.6023/a20080399
20. **Gao, Y.G., Huangfu, S.Y., Patil, S., Tang, Q., Sun, W., Li, Y., Lu, Z., Qian, A.** [12]aneN_3-based Multifunctional Compounds as Fluorescent Probes and Nucleic Acids Delivering Agents *Drug Delivery* 27 (1) 2020: pp. 66 – 80. https://doi.org/10.1080/10717544.2019.1704943
21. **Saito, G., Velluto, D., Resmini, M.** Synthesis of 1, 8-naphthalimide-based Probes with Fluorescent Switch Triggered by Flufenamic Acid *Royal Society Open Science* 5 (6) 2018: pp. 88 – 91. https://doi.org/10.1098/rsos.172137
22. **Shangguan, M., Jiang, X., Lu, Z., Zou, W., Chen, Y., Xu, P., Pan, Y., Hou, L.** A coumarin-based Fluorescent Probe for Hypochlorite Ion Detection in Environmental Water Samples and Living Cells *Talanta* 202 2019: pp. 303 – 307. https://doi.org/10.1016/j.talanta. 2019.04.074
23. **Jin, Y., Liu, R., Zhan, Z., Lv, Y.** Fast Response Near-infrared Fluorescent Probe for Hydrogen Sulfide in Natural Waters *Talanta* 202 2019: pp. 159 – 164. https://doi.org/10.1016/j.talanta.2019.04.067
24. **Gong, H.H., Addla, D., Lv, J.S., Zhou, C.H.** Heterocyclic Naphthalimides as New Skeleton Structure of Compounds with

Increasingly Expanding Relational Medicinal Applications *Current Topics in Medicinal Chemistry* 16 2016: pp. 3303 – 3364. https://doi.org/10.2174/15680266 16666160506145943

25. **Zhang, S.Z., Gu, Y.L., Shi, Z.Q., Lu, N., Xu, H.Y.** A Novel Reversible Fluorescent Probe Based on Naphthalimide for Sequential Detection of Aluminum (Al^{3+}) and Fluoride (F^{-}) Ions and its Applications *Analytical Methods: Advancing Methods and Applications* 13 (44) 2021: pp. 5360 – 5368. https://doi.org/10.1039/D1AY01545A
26. **Wang, F., Xu, Y., Aderinto, S.O., Peng, H., Zhang, H., Wu, H.** A New Highly Effective Fluorescent Probe for Al^{3+} Ions and its Application in Practical Samples *Journal of Photochemistry & Photobiology, A: Chemistry* 332 2017: pp. 273 – 282. https://doi.org/10.1016/j.jphotochem.2016.09.004
27. **Zhang, P., Guo, X., Xiao, Y., Xiao, Y., Zhang, Q., Ding, C**. Twisted Intramolecular Charge Transfer (TICT) Based Fluorescent Probe for Lighting up Serum Albumin with High Sensitivity in Physiological Conditions *Spectrochimica Acta Part A: Molecular and Biomolecular Spectroscopy* 223 2019: pp. 117318. https://doi.org/10.1016 /j.saa.2019.117318
28. **Gao, C., Liu, X., Chen, W., Wang, F., Jiang, J.** A Naphthalene-based Fluorescent Probe for Ratiometric Imaging of Lysosomal Hydrogen Sulfide in Living Cells *Methods and Applications in Fluorescence* 7 (1) 2018: pp. 014002. https://doi.org/10.1088/2050-6120/aae9c4
29. **Qiao, Q.L., Liu, W., Chen, J., Zhou, W., Yin, W., Lu, M., Cui, J., Xu, Z.C.** A Naphthalimidederived Fluorogenic Probe for SNAP-tag with a Fast Record Labeling Rate *Dyes and Pigments* 147 2017: pp. 327 – 333. https://doi.org/10.1016/j.dyepig.2017.08.032
30. **Luo, X., Wu, W., Deng, F., Chen, D., Luo, S., Au, C.** Quantum dot-based turn-on Fluorescent Probe for Imaging Intracellular Zinc(II) and Cadmium(II) Ions *Microchimica Acta* 181 (11 – 12) 2014: pp. 1361 – 1367. https://doi.org/10.1007/s00604-014-1264-z
31. **Xu, H., Miao, R., Fang, Z., Zhong, X.** Quantum Dot-based "turn-on" Fluorescent Probe for Detection of Zinc and Cadmium Ions in Aqueous Media *Analytica Chimica Acta* 687 (1) 2010: pp. 82 – 88. https://doi.org/10.1016/j.aca.2010.12.002
32. **Singh, D., Thakur, N., Raj, K.K., Pandey, R.** Development of Aminoethylpyridine Based N, N, N, O-donor Fluorescent Probes for the Detection of Fe^{3+} and Hg^{2+} in Aqueous Media *Journal of Physics: Conference Series* 1504 (1) 2020: pp. 012001. https://doi.org/10.1088/1742-6596/1504/1/012001
33. **Liu, Y., Gao, S., Yang, L., Liu, Y.L., Liang, X.M., Ye, Fei., Fu, Y.** A Highly Selective Perylenediimide-Based Chemosensor: "Naked-Eye" Colorimetric and Fluorescent Turn-on Recognition for $Al^{3+}$and its Application in Practical Samples, Test Paper and Logic Gate *Frontiers in Chemistry* 8 (1) 2020: pp. 347 – 357. https://doi.org/10.1007/s10895-017-2197-9
34. **Zheng, L., Cheng, Z., He, H., Xu, H., Liang, F., Pang, L.** Ion Recognition and Fluorescent Imaging of Conjugated Polymer Fuorescent Probes for Fe(III) *Bulletin of Materials Science: Published by the Indian Academy of Sciences* 43 (1) 2020: pp. 87 – 90. https://doi.org/10.1007/s12034-019-2029-4
35. **Kang, L., Xing, Z.Y., Ma, X.Y., Liu, Y.T., Zhang, Y.** A Highly Selective Colorimetric and Fluorescent Turn-on Chemosensor for Al^{3+} Based on Naphthalimide Derivative *Spectrochimica Acta Part A: Molecular and Biomolecular Spectroscopy* 167 2016: pp. 59 – 65. https://doi.org/10.1016/j.saa.2016.05.030
36. **Kang, L., Liu, Y.T., Li, N.N., Dang, Q.X., Xing, Z.Y., Li, J.L., Zhang, Y.** A Schiff-base Receptor Based Naphthalimide Derivative: Highly Selective and Colorimetric Fluorescent Turn-on Sensor for Al^{3+} *Journal of Luminescence* 186 2017: pp. 48 – 52. https://doi.org/10.1016/j.jlumin.2016.12.056
37. **Silva, A.P.D., Fox, D.B., Moody, T.S., Weir, S.M.** The Development of Molecular Fluorescent Switches *Trends in Biotechnology* 19 (1) 2001: pp. 29 – 34. https://doi.org/10.1016/s0167-7799(00)01513-4
38. **Rurack, K., Danel, A., Rotkiewicz, K., Grabka, D., Spieles, M., Rettig, W.** 1, 3-Diphenyl-1H-pyrazolo[3, 4-b]quinoline: a Versatile Fluorophore for the Design of Brightly Emissive Molecular Sensors *Organic Letters* 4 (26) 2002: pp. 4647 – 4650. https://doi.org/10.1021/ol027025i
39. **Biswas, S., Sharma, V., Kumar, P., Koner, A.L.** Selective Sensing of Lysosomal Iron(III) Via Three-component Fluorescence-based Strategy in Living Cells *Sensors & Actuators: B. Chemical* 260 2018: pp. 460 – 464. https://doi.org/10.1016/j.snb.2018.01.011
40. **Huang, L., Chen, Y., Zhao, Y., Wang, Y., Xiong, J., Zhang, J., Wu, X., Zhou, Y.** A Ratiometric Near-infrared Naphthalimide-Based Fluorescent Probe with High Sensitivity for Detecting Fe^{2+} in Vivo *Chinese Chemical Letters* 31 (11) 2020: pp. 2941 – 2944. https://doi.org/10.1016/j.cclet.2020.06.006
41. **Jothi, D., Munusamy, S., Sawminathan, S., Iyer, S.K.** Highly Sensitive Naphthalimide Based Schiff Base for the Fluorimetric Detection of Fe^{3+} *RSC Advances* 11 (19) 2021: pp. 11338 – 11346. https://doi.org/10.1039/d1ra 003 45c